Ferroelectric Domains in Multiferroic $BiFeO_3$ Films under Epitaxial Strains

Wei Ren,[1,2,*] Yurong Yang,[2,3] Oswaldo Diéguez,[4,5] Jorge Íñiguez,[4] Narayani Choudhury,[2,6] and L. Bellaiche[2]

[1]*Department of Physics, Shanghai University, 99 Shangda Road, Shanghai 200444, China*
[2]*Physics Department and Institute for Nanoscience and Engineering, University of Arkansas, Fayetteville, Arkansas 72701, USA*
[3]*Physics Department, Nanjing University of Aeronautics and Astronautics, Nanjing 210016, China*
[4]*Institut de Ciència de Materials de Barcelona (ICMAB-CSIC), Campus UAB, 08193 Bellaterra, Spain*
[5]*Department of Physics and Astronomy, Rutgers University, Piscataway, New Jersey 08854, USA*
[6]*Center for University Programs, University of Washington, Bothell, Washington 98011, USA*

(Received 18 September 2012; published 3 May 2013)

First-principles calculations are performed to investigate energetic and atomistic characteristics of ferroelectric domains walls (DWs) of $BiFeO_3$ (BFO) films subject to compressive strain. Significantly lower DW energies than those previously reported, and a different energetic hierarchy between the various DW types, are found for small strains. In all investigated cases (corresponding to ideal angles of 71°, 109°, and 180° formed by the domain polarizations), the DW energy reaches its maximum value for misfit strains that are around the critical strain at which the transition between the *R*-like and *T*-like phases occurs in single-domain BFO. Near these strains, several quantities depend strongly on the type of domain wall; such distinct behavior is associated with an elastic difference and a large out-of-plane polarization at the DW in the 180° case. A further increase of the magnitude of the strain leads to (i) a change of hierarchy of the DW energies, (ii) large out-of-plane polarizations inside each up and down domain, and (iii) novel atomic arrangements at the domain walls. Our study can thus initiate a new research direction, namely strain engineering of domain-wall functionalities.

DOI: 10.1103/PhysRevLett.110.187601 PACS numbers: 77.80.Dj, 77.55.Nv, 77.80.bn

Domain walls (DWs) separating different ferroelectric domains have been ubiquitously observed in experiments in many compounds [1], and form to minimize elastic and electrostatic energies. Such domains and their walls have a profound influence on physical properties of ferroelectrics. For example, they are promising for a wide range of practical uses, including nonvolatile random access memories [2] and piezoelectric devices [3]. Fundamental studies of electronic transport [4,5] and above-band gap photovoltaic properties [6,7] based on domain walls in $BiFeO_3$ (BFO) thin films have also been reported very recently with great potential of applications.

On another topic, epitaxial strain (arising from the lattice mismatch between film and substrate) is also known to dramatically affect multiferroic properties of *single-domain* BFO systems, even leading to emergence of many desirable effects [8–12]. For instance, it is now well understood that epitaxial compressive strain (with a magnitude larger than 4.4%) can induce a polarization rotation from [111] to nearly [001], accompanied by the appearance of a huge c/a tetragonal ratio of about 1.3 and fivefold coordinated Fe atoms [13–15], in (001)-oriented monodomains of BFO.

Interestingly, while energetic and atomistic characteristics of different domain walls have been studied in BFO bulks [16], these quantities and their evolutions with the magnitude of the misfit strain are completely unknown in BFO films subject to epitaxial strains, despite their obvious importance. The goal of this Letter is to fill this paucity of knowledge, by investigating the effect of strain on properties of different domain walls in epitaxial BFO films (Note also that it is highly likely that different experimental groups will observe different domains or a different averaging between domains, especially if they use different growth techniques or procedures or different substrates. This explains why we will report and discuss here properties of three different walls for a large range of strain.) As we will see, many novel effects are presently found, and the concept of strain engineering of domain-wall functionalities is demonstrated as a new advance based on the well-studied engineering of domain wall configurations [1,17].

Two different kinds of epitaxial (001) BFO films are investigated: one possessing a single domain (SD) structure *versus* one exhibiting a multidomain (MD) configuration. For the SD case, we use a 10-atom supercell (that is described in the Supplemental Material [18]) for which the in-plane and out-of-plane lattice pseudocubic constants are denoted by a and c, respectively. The misfit strain is thus defined as $(a - a_0)/a_0$, where a_0 corresponds to the pseudocubic lattice parameter of BFO bulk (which is equal to 3.9 Å according to our first-principles simulations). Regarding the MD structures, we investigate three different cases corresponding (at small misfit strain) to 109°, 71°, and 180° domain walls. These three cases are denoted as DW109, DW71, and DW180, respectively, and correspond to the three possible angles that the polarization of the "up" domains makes with the polarization of the "down" domains if both of them lie along two different ⟨111⟩

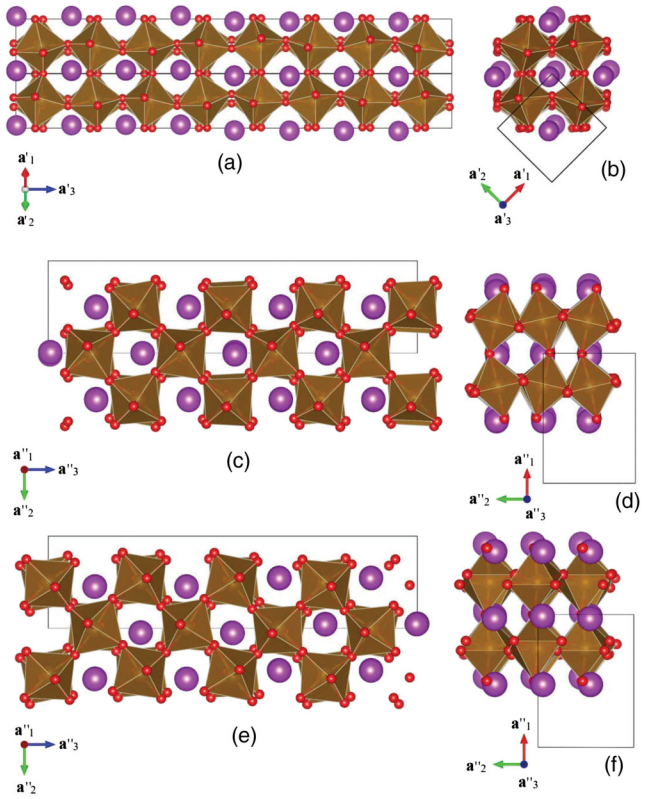

FIG. 1 (color online). Schematic models for (a), (b) 109°; (c), (d) 71°; and (e),(f) 180° multidomain structures. Purple spheres represent Bi atoms, and FeO_6 octahedra are illustrated by brown units.

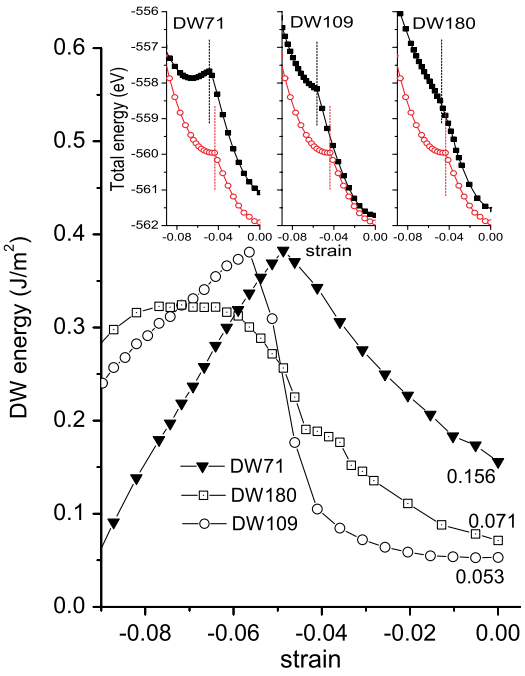

FIG. 2 (color online). Dependence of domain wall energies on the in-plane epitaxial strain for the investigated multidomain structures. The insets show the minimum total energy of the MD structures (in solid black squares) and SD configurations (via open red circles) as a function of the misfit strain. In these insets, the vertical dashed lines delimit the strain regions for which the MD structures adopt an *R*-like phase while the SD configuration has already transformed into its *T* phase.

directions. Note that up (respectively, down) terminology refers to domains for which the *out-of-plane* polarization is parallel (respectively, antiparallel) to the [001] pseudocubic axis. As schematized in Figs. 1(a) and 1(b), an 80-atom supercell is used to mimic DW109, and has the following lattice vectors: $\mathbf{a}'_1 = (0, a, c)$, $\mathbf{a}'_2 = (0, -a, c)$, $\mathbf{a}'_3 = (8a, 0, \delta)$. These lattice vectors are nearly oriented along the pseudocubic [011], [0-11], and [100] directions when $a = c$ (which occurs for small misfit strain). They allow the up and down domains to propagate along the [100] direction—because the change in polarization between the two domains should be perpendicular to the domain propagation direction [19–21]. (Note that the polarizations of the two different domains in the DW109 case nearly lie along [111] and [1-1-1] at small misfit strain.) For both the DW71 and DW180 cases, we adopted another 80-atom supercell that is shown in Figs. 1(c)–1(f) and that possesses the following lattice vectors: $\mathbf{a}''_1 = (\delta_1, \delta_2, 2c)$, $\mathbf{a}''_2 = (a\sqrt{2}, 0, 0)$, $\mathbf{a}''_3 = (0, 4a\sqrt{2}, 0)$, where δ_1 and δ_2 are parameters (typically having small values) to be relaxed for each studied in-plane lattice parameter, a. These vectors are nearly oriented along the [001], [110], and [-110] pseudocubic directions, respectively, for small misfit strain, and the up and down domains alternation along the [-110] pseudocubic direction. The polarizations, at small misfit strain, in the two different kinds of domains are nearly along [-111] and [-11-1] for DW71, while they are close to [111] and [-1-1-1] for DW180. All the supercells used here allow the incorporation of both the *G*-type antiferromagnetic order of Fe ions and antiferrodistortive (AFD) motions associated with antiphase oxygen octahedral tiltings [22–25]. More details about the MD structures are provided in the Supplemental Material [18]. Technically, our calculations are performed using the Vienna *ab initio* simulation package (VASP) code [26,27] for both the SD and MD cases. See the Supplemental Material for a more detailed description of such computations [18]. Note that the domains considered here are of the nanoscale.

Figure 2 shows the predicted energy density of each considered MD structure, as a function of the misfit strain. This density is conventionally referred to as the DW energy and is defined as $\varepsilon_{DW} = (E_{MD} - E_{SD})/2A$. Here, A is the total area of the domain walls, and is therefore equal to $2ac$ for DW109 and $2\sqrt{2}ac$ for both DW71 and DW180. E_{MD} and E_{SD} are the *minimum* total energies (per 80 ions) of the MD and SD structures having the same in-plane lattice parameter, respectively, and are shown in the insets of Fig. 2.

Let us first concentrate on the results at low misfit strain. The DW109, DW180, and DW71 cases show minimal wall

energies of 0.053 J/m^2, 0.071 J/m^2, and 0.156 J/m^2, respectively. These results are very similar to the ones obtained by Dieguez *et al.* [28] who have studied DW configurations in bulk BFO, including those that are analogous to the ones analyzed here. In agreement with Ref. [16], DW109 is found to be the energetically most stable domain among the three considered MD cases. However, unlike in Ref. [16], but in agreement with more recent works [28,29], the least stable MD is found here to be DW71 rather than DW180. Furthermore, our magnitudes of ε_{DW} for the zero misfit strain are *significantly* smaller than the values of 0.205, 0.363, and 0.829 J/m^2 for the 109°, 71°, and 180° domain walls, respectively, reported in Ref. [16]. Let us note that our calculations are technically very similar to those of Ref. [16], and we explicitly checked that the small difference in calculation parameters (e.g., plane-wave cutoff, etc.) cannot account for the differences in the computed DW energies, in line with the conclusions of Ref. [28]. Hence, we tend to believe that the results of Ref. [16] correspond to atomic DW configurations that are local minima of the energy; as discussed in Ref. [28], the possibility of getting trapped in such high-lying minima is not a rare one when working with $BiFeO_3$, given Bi's ability to form many competitive local coordinations. Naturally, because the DW energies found in the present work, as well as in Refs. [28,29], are much lower than those reported in Ref. [16], our results are more likely to be of physical significance. It is noteworthy that the experimentally domain wall energy for $BiFeO_3$ on (001) $SrTiO_3$ substrate was found to be approximately 0.1 J/m^2, which is consistent with our present predictions [30]. Also, it has been experimentally reported [30–33] that BFO films tend to display 71 DWs more frequently, which does not seem consistent with our computed energies. In our opinion, this clearly suggests that additional factors, not present in our calculations, play an important role in the real samples—e.g., growth conditions, defects and imperfections, interfaces with substrate and/or electrodes, electric boundary conditions, etc. (see, e.g., Sec. III.D of Ref. [28] for a discussion of some of these effects).

As regards the atomic structure of our domain walls, we observed that the discontinuity of both polar and AFD distortions is very sharp. Interestingly, the relaxed DWs seem to owe their relatively low energy to the good matching of the O_6 rotations at the plane of the wall, which is such that the deformation of the octahedra is minimal. This observation coincides with the conclusions of Ref. [28], where these structural aspects for the bulk DWs are discussed in more detail.

We now turn our attention to the impact of epitaxial strains on the total and DW energies for the three investigated MD cases, which constitutes an important and novel result. For that, let us first emphasize that the insets of Fig. 2 show a significant change in slope of the total energy *versus* in-plane lattice constant curve at a misfit strain of −4.4% for *monodomain* BFO. Such change is caused by a first-order phase transition separating the so-called *R*-like and *T*-like BFO phases, in agreement with previous studies [13,14]. Interestingly, the insets of Fig. 2 also reveal that a noticeable change of curvature of the total energy occurs for DW71 and DW109, but at different misfit strains, namely −4.9% and −5.6%. As we will see later, such a difference in critical strains with respect to the SD case implies that the *T*-*R* transition occurs at higher misfit strain *inside each domain* for these two latter MDs. Such a difference is also related to the nanoscale dimension of our investigated domains. Moreover, the total energy *versus* misfit strain also changes the curvature around −4.6%, but in a much less pronounced way, in the DW180 case. Note that our notations DW71, DW109, and DW180 for domains walls are still used (in reference to the DW structures at small misfit strain) even if the angle between polarizations of neighboring domains can be strongly strain dependent.

The difference between the minimal total energies of the MD and SD structures gives rise to interesting behaviors of the DW energies when the misfit strain increases from its zero value. First of all, and as shown in Fig. 2, all three DW energies increase with compressive strain [34]—which is due to the fact that, in the *R*-like region, the total energy increases faster with compressive strain in the MD cases than it does for the SD configuration. Then, ε_{DW} of DW109 and DW71 peak at misfit strains of −5.6% and at −4.9%, respectively, for which the domains inside these MD configurations are at the border between the *T*-to-*R* phase transition while the SD has already transformed into its *T* phase. On the other hand, DW180 shows a distinct plateau under strains between −6% and −8%. Such a plateau reflects the fact that the energies of the *T* phase of the DW180 and SD cases have approximately the same dependency with the misfit strain for compressive strain above 6% in magnitude. Interestingly, in the highly strained regime, the energy of DW71 considerably decreases when further increasing the misfit strain. This occurs because the total energy of the *T*-like phase in the SD case significantly increases with the strain magnitude, while that of DW71 adopts a minimum at around 6.5%. Such a decrease results in (i) an even lower value of ε_{DW} of DW71 for compressive strains beyond 8% than for a zero misfit strain; and (ii) a change in hierarchy, with respect to that at zero misfit strain, of the DW energies: at large compressive strain, DW71 is now more stable than DW109 and DW180.

Figure 3 also reports various properties of the MD structures as a function of the misfit strain. These properties are the c/a axial ratio [Fig. 3(a)], the Cartesian components of the polarization in the up (solid symbols) and down (open symbols) domains [Fig. 3(b)], and the average angle made by these two different polarizations [Fig. 3(c)]. We observe in Fig. 3(a) that the axial ratio generally increases with the

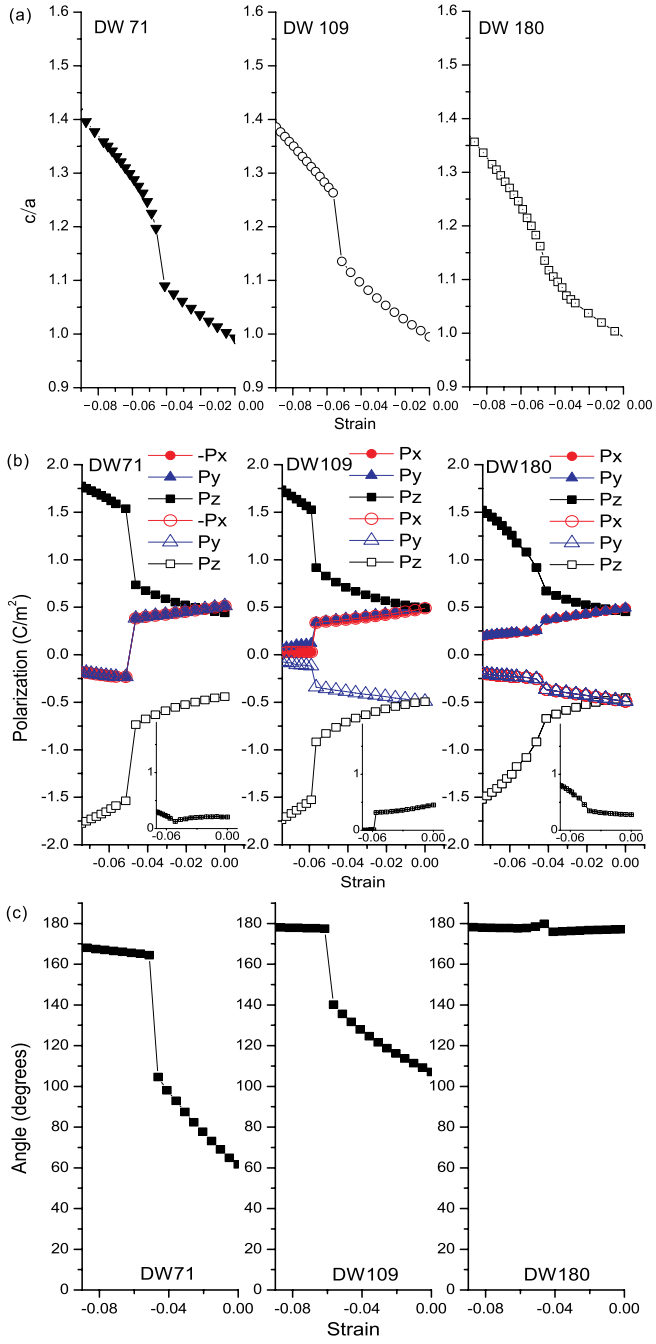

FIG. 3 (color online). Properties of multidomain structures as a function of the epitaxial strain. Panel (a) shows the axial ratio between the long and short axes of the pseudocubic unit cell. Panel (b) displays the Cartesian components of the polarization in the up (solid symbols) and down (open symbols) domains. Panel (c) represents the average angle formed by these two different polarizations. Insets of panel (b) display the average *magnitude* of the out-of-plane component of the polarization at the domain walls.

compressive strain, and giant values (greater than 1.3) can be achieved under ultrahigh strain. For DW71 and DW109, such increases appear to occur abruptly with a jump near the critical strain. In contrast, a smoother transition is observed for DW180. As a consequence of the structural change and growing axial ratios when increasing the strength of the misfit strain, the polarization in each up and down domain within the DW71, DW109, and DW180 structures rotate from a pseudocubic ⟨111⟩ direction towards the [001] (for the up domains) or [00-1] (for the down domains) direction. There is a large change in polarization close to the critical strains, and the resulting out-of-plane component is anomalously large for higher strains in the three investigated MDs. These behaviors of the axial ratio and polarization are reminiscent of the R-to-T transition in monodomain BFO [13,14]. It is a remarkable fact that even at very large compressive strain, there is still significant amount of polarization being in plane for DW71 and DW180. On the other hand, the suppression of in-plane polarization is nearly complete for DW109 at the largest investigated strains (this suppression occurs around a misfit strain of -8% for the SD case). Similar to the corresponding structures at zero-misfit strain, the in-plane polarization is homogenous in DW71, whereas for DW180 the in-plane polarizations are antiparallel between the two neighboring domains (they are along the [110] and [-1-10] directions, respectively; that is, they are both inside the plane containing the DW); finally, for DW109 the in-plane components make a 90° zigzag domain structure for any strain, since they are oriented along the [110] and [1-10] directions for the up and down domains, respectively. Furthermore, for DW71, the angle between the polarization vectors of the up and down domains increases rapidly with strain up to 105° before the transition strain at -4.9%, followed by an abrupt jump to about 165°. DW109 has a similar trend, but reaches 180° for the largest investigated strain (as a result of the nearly vanishing of the in-plane components of the polarization in the domains). In contrast, for the DW180 case this angle shows that the overall polarizations of the up and down domains are always antiparallel to each other, when the strain is below and beyond the critical value.

We have also computed the elastic stiffness constants, C_{ijkl} [35]. In particular, we found that C_{3333} (where the 3 index is along the alternating direction of the domains) is of the order of 500 GPa for all the MD configurations, for either a compressive strain of -2.5% (R-like phase) or of -7.7% (T-like phase). The only exception to this rule is the high-strain phase of DW180: as a matter of fact, this phase presents a much smaller value of this coefficient, of the order of 300 GPa, for the compressive strain of -7.7%. Hence, the R-to-T transition in DW180 is connected to a distinct elastic behavior of its high-strain phase. Further, as indicated in the insets of Fig. 3(b), the T phase of DW180 also exhibits an unusually large magnitude of the out-of-plane polarization [36] (that further increases as the compressive strain grows in strength) at *the domain walls*.

More details about the MD structures, such as an unusual atomic arrangement at the DW for large strains and its electronic densities of states, are also provided in

the Supplemental Material [18]. The large changes in domain wall energies found in our study may have many implications for the properties of ferroelectric thin films such as domain shape, domain wall motion, switching coercive fields, photovoltaic and conductivity properties. An obvious example of such physical quantity is the polarization-versus-electric field hysteresis loop, because the magnitude of the electric field needed to transform the multidomains into a monodomain crucially depends on the domain wall energy (since this latter is precisely the difference in energy between a multidomain and a monodomain). We therefore hope that our study is of benefit to scientists interested in nanoscience, phase transitions, and multiferroics. It can be considered as an example of an exciting and, novel research direction, namely strain engineering of domain-wall functionalities.

This work is mostly supported by ARO Grant No. W911NF-12-1-0085. We acknowledge the Department of Energy, Office of Basic Energy Sciences, under Contract No. ER-46612, NSF Grants No. DMR-1066158 and No. DMR-0701558, and ONR Grants No. N00014-12-1-1034, No. N00014-11-1-0384, and No. N00014-08-1-0915 for discussions with scientists sponsored by these grants. Some computations were also made possible thanks to the MRI Grant No. 0722625 from NSF, Shanghai Supercomputer Center, the ONR Grant No. N00014-07-1-0825 (DURIP), and a Challenge grant from the Department of Defense. We also acknowledge the Eastern Scholar Program of the Shanghai Municipal Education Commission, the support from National Natural Science Foundation of China under Grant Nos. 11274222 and 51032002, Shanghai Shuguang Program (12SG34), and the 863 Program of China (No. 2011AA050526). O. D. and J. I. acknowledge funding from MINECO-Spain [Grants No. MAT2010-18113, No. MAT2010-10093-E, and No. CSD2007-00041, and the ''Ramón y Cajal'' program (O. D.)].

*renwei@shu.edu.cn

[1] G. Catalan, J. Seidel, R. Ramesh, and J. F. Scott, Rev. Mod. Phys. **84**, 119 (2012).
[2] A. Q. Jiang, C. Wang, K. J. Jin, X. B. Liu, J. F. Scott, C. S. Hwang, T. A. Tang, H. B. Lu, and G. Z. Yang, Adv. Mater. **23**, 1277 (2011).
[3] J. X. Zhang *et al.*, Nat. Nanotechnol. **6**, 98 (2011).
[4] P. Maksymovych, J. Seidel, Y. H. Chu, P. Wu, A. P. Baddorf, L.-Q. Chen, S. V. Kalinin, and R. Ramesh, Nano Lett. **11**, 1906 (2011).
[5] N. Balke *et al.*, Nat. Phys. **8**, 81 (2011).
[6] T. Choi, S. Lee, Y. J. Choi, V. Kiryukhin, and S.-W. Cheong, Science **324**, 63 (2009).
[7] M. Alexe and D. Hesse, Nat. Commun. **2**, 256 (2011).
[8] I. C. Infante *et al.*, Phys. Rev. Lett. **105**, 057601 (2010).
[9] S. Prosandeev, I. A. Kornev, and L. Bellaiche, Phys. Rev. Lett. **107**, 117602 (2011).
[10] C. Daumont *et al.*, J. Phys. Condens. Matter **24**, 162202 (2012).
[11] W. Chen *et al.*, Appl. Phys. Lett. **99**, 222904 (2011).
[12] Y. Yang, W. Ren, M. Stengel, X. H. Yan, and L. Bellaiche, Phys. Rev. Lett. **109**, 057602 (2012).
[13] B. Dupé, I. C. Infante, G. Geneste, P.-E. Janolin, M. Bibes, A. Barthélémy, S. Lisenkov, L. Bellaiche, S. Ravy, and B. Dkhil, Phys. Rev. B **81**, 144128 (2010).
[14] A. J. Hatt, N. A. Spaldin, and C. Ederer, Phys. Rev. B **81**, 054109 (2010).
[15] Z. Chen *et al.*, Phys. Rev. B **84**, 094116 (2011).
[16] A. Lubk, S. Gemming, and N. A. Spaldin, Phys. Rev. B **80**, 104110 (2009).
[17] E. K. H. Salje, ChemPhysChem **11**, 940 (2010).
[18] See Supplemental Material at http://link.aps.org/supplemental/10.1103/PhysRevLett.110.187601 for further computational and technical details.
[19] S. K. Streiffer, C. B. Parker, A. E. Romanov, M. J. Lefevre, L. Zhao, J. S. Speck, W. Pompe, C. M. Foster, and G. R. Bai, J. Appl. Phys. **83**, 2742 (1998).
[20] W. J. Merz, Phys. Rev. **95**, 690 (1954).
[21] J. Fousek and V. Janovec, J. Appl. Phys. **40**, 135 (1969).
[22] W. Ren and L. Bellaiche, Phys. Rev. Lett. **107**, 127202 (2011).
[23] D. Sichuga, W. Ren, S. Prosandeev, and L. Bellaiche, Phys. Rev. Lett. **104**, 207603 (2010).
[24] W. Ren and L. Bellaiche, Phys. Rev. B **82**, 113403 (2010).
[25] D. Albrecht, S. Lisenkov, W. Ren, D. Rahmedov, I. A. Kornev, and L. Bellaiche, Phys. Rev. B **81**, 140401 (2010).
[26] G. Kresse and J. Furthmüller, Phys. Rev. B **54**, 11169 (1996).
[27] G. Kresse and D. Joubert, Phys. Rev. B **59**, 1758 (1999).
[28] O. Diéguez, P. Aguado-Puente, J. Junquera, and J. Íñiguez, Phys. Rev. B **87**, 024102 (2013).
[29] Y. Wang *et al.*, *Proceedings of the Materials Science and Technology Conference, Columbus, Ohio, 2011* (ASM International, Materials Park, OH, 2011).
[30] Y. B. Chen, M. B. Katz, X. Q. Pan, R. R. Das, D. M. Kim, S. H. Baek, and C. B. Eom, Appl. Phys. Lett. **90**, 072907 (2007).
[31] C. J. M. Daumont, S. Farokhipoor, A. Ferri, J. C. Wojdeł, J. Íñiguez, B. J. Kooi, and B. Noheda, Phys. Rev. B **81**, 144115 (2010).
[32] Y. H. Chu *et al.*, Adv. Mater. **18**, 2307 (2006).
[33] C. A. Randall, D. J. Barber, and R. W. Whatmore, J. Mater. Sci. **22**, 925 (1987).
[34] S. P. Beckman, X. Wang, K. M. Rabe, and D. Vanderbilt, Phys. Rev. B **79**, 144124 (2009).
[35] J. Nye, *Physical Properties of Crystals: Their Representation by Tensors and Matrices* (Oxford University Press, New York, 1985).
[36] S. Poykko and D. J. Chadi, Appl. Phys. Lett. **75**, 2830 (1999).